The density of supercooled water. II. Bulk samples cooled to the homogeneous nucleation limit

D. E. Hare and C. M. Sorensen
Department of Physics, Kansas State University, Manhattan, Kansas 66506

(Received 1 December 1986; accepted 17 July 1987)

We have measured the density of supercooled water (H_2O) in the range $-33.41 \leqslant T \leqslant -5.23$ °C. Our samples were held in glass capillary tubing with an approximate inside diameter of 0.3 mm = 300 μ. These samples were prepared by Mossop's method and could be cooled to their homogeneous nucleation limit before freezing. We compare our density data to other measurements using capillaries and demonstrate what appears to be an excess density in smaller capillaries which is inversely proportional to the capillary inside diameter. The origins of this excess density are unknown, but we show its effect is insignificant on our measurement. The thermal expansivities derived from our data are fit to a power law in temperature relative to a singular temperature. These results are inconclusive due to a poor knowledge of the background expansivity.

I. INTRODUCTION

Water's unusual physical properties are well known. Speedy and Angell[1] showed that when water is supercooled many of these properties behave as if approaching a singularity at $T_s \simeq -45$ °C. This has stimulated considerable experimental and theoretical effort to explain these anomalies.[2,3] Perhaps the best known anomalous property of water is its density which displays a maximum at 4 °C. The rapid decrease in density at yet lower temperatures is important because it is a manifestation of the open, hydrogen bonded network structure of liquid water which is thought to dominate the physical properties in the supercooled regime.

Much of the experimental work on supercooled water has been performed on small samples confined in either capillaries or emulsion droplets. Leyendekkers and Hunter[4] have argued that the effect of surface energy on the free energy of these small samples can be considerable, especially for samples in the micron size range. They also argued that overestimates of the magnitude of some of the anomalous properties have been made due to these surface effects and that the apparent anomalous temperature might be closer to -60 °C.

In the first paper in this series we presented density data for both H_2O and D_2O in 25 μ i.d. capillaries.[5] We concluded that earlier work probably had overestimated the magnitude of the anomalous part of the thermal expansivity as Leyendekkers and Hunter had proposed. We could not, however, support a new singular temperature due to ambiguity in the background part of the expansivity, and the somewhat arbitrary nature of such a fit. This problem still remains.

The main purpose of this paper is to present the coldest possible, bulk sample data for the density of H_2O. To do this we have made capillary samples of water using Mossop's[6] technique which have an inside diameter of roughly 0.3 mm (300 μ). These samples can be cooled to the homogeneous nucleation limit, nature's limit for the coldest possible temperature for a substance to remain liquid. Comparison of our results with earlier density measurements in capillaries shows the density to be dependent on the capillary size. The excess density relative to the bulk density is inversely proportional to the capillary inside diameter and increases exponentially with decreasing temperature. We do not believe that this excess density is related to an excess surface energy as proposed by Leyendekkers and Hunter. We can justify that our density data presented here are in the bulk limit, essentially free of these small capillary effects. We then use these data to calculate the thermal expansivity and test the power law behavior of the expansivity.

II. EXPERIMENTAL METHOD

To achieve supercooling of bulk samples to the homogeneous nucleation limit, we used Mossop's method[6] to make our samples. Our Mossop apparatus consisted of a one liter flask with a stopcock valve at the top and a side tube off the flask neck. This side tube was attached via an O-ring seal to our capillary stock tubing which was made of standard Pyrex tube with 3 mm i.d. and 5 mm o.d. and hung vertically downward.

To make our samples the flask and tubing were thoroughly cleaned and the flask was nearly completely filled with filtered, distilled water on a clean bench. The water was then boiled for roughly 2 1/2 h until about 250 ml of water remained in the flask. The stopcock valve was closed during this boiling to allow for vigorous emission of steam out through the capillary stock tubing. Our experience indicated that nearly complete filling and prolonged boiling helped rid the system of potential nucleating particles. Next the stopcock was opened sufficiently to reduce the pressure in the flask so that steam passed only slowly out of the capillary stock tubing. Samples were then made by pulling the 5 mm stock tubing in an oxymethane flame down to roughly 0.5 mm outside diameter. The lower end was then fused shut and the pure vapor was allowed to condense from above. When a sufficient amount of liquid had condensed, the tube was carefully fused shut at the top. Samples were carefully scrutinized at the ends and rejected if there seemed to be the smallest possibility of a microleak.

 0021-9606/87/204840-06$02.10

A properly made tube was about 10 cm long, having an outside diameter of roughly 0.5 mm and an inside diameter of roughly 0.3 mm with no microleaks at either end. The entire interior volume was filled with liquid except for a small space of approximately 5 mm length at one end. This space contained virtually pure water vapor with no air.

About 30% of all the samples that we judged "properly made" could be cooled to -31 °C and held there for 10 min during a preliminary rejection run. Of those that survived this first run, about 60% would eventually yield useable data.

The densities were measured in a manner similar to our earlier work.[5] The samples were mounted on a clear plastic slide and placed in a methanol filled temperature control bath. The measurement we made on a sample was the distance from the meniscus to the top of the tube's interior. Let this distance be referred to as Y as illustrated in Fig. 1. Y was measured using a long working distance, 2.6 power microscope equipped with a filar micrometer. The collection of raw data consisted of gathering (temperature, Y) ordered pairs for each tube. Those pairs for which $T>0$ °C could also be associated with known densities taken from Kell.[7] With knowledge of (temperature, Y, density) triplets it was possible to calibrate the tube so that we could obtain our densities from our raw data, corrected for Pyrex expansion. This calibration of known densities to Y for $T>0$ °C eliminated any problems regarding nonuniform inside diameters of the Mossop tubes. Surprisingly, we found the cross sectional areas of the tubes were uniform to much better than 1 part in 10^4, although such uniformity was not necessary due to the calibration. Raw densities were calculated to five significant figures.

Evaporation of the main bead and recondensation on the sidewalls of the vapor space caused us serious problems in accuracy and reproducibility of data in our initial experiments. This problem was remedied by placing a small, low powered heater near the vapor space to keep it slightly warmer than the rest of the sample. This method was carefully examined for its effect on uniformity of sample temperature and found not to cause significant error in our measurements. Its use was not necessary below -10 °C.

Temperature was controlled to ± 0.01 °C with the aid of a Neslab EX-300DD bath modified to accept mechanical refrigeration probes. Temperatures were measured with an accuracy of ± 0.01 °C with mercury-in-glass, NBS traceable thermometers.

Ten different capillary samples yielded useful data to below -30 °C. Three samples went below -33 °C. Mossop concluded that these temperatures represented homogeneous nucleation temperatures for samples of this size. Density data for the samples are given in Table I to four significant figures.

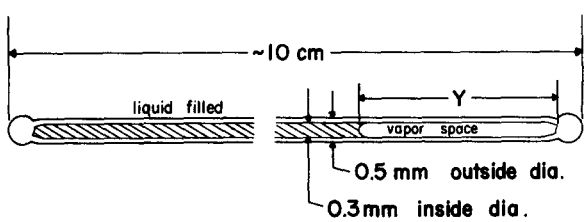

FIG. 1. Drawing of the capillary sample tube.

III. ANALYSIS AND DISCUSSION

We first fit our density data in Table I to a polynomial in temperature. This fit included both our data set from $-33.41<T<-5.23$ °C and higher accuracy data from Kell[7] in the range $-4<T<10$ °C. The Kell data were included so our fit would reflect the density maximum. The lowest order polynomial that could fit our data without any significant systematic deviations was a sixth-order polynomial given by

TABLE I. Raw density data.

T (°C)	Density (g/ml)	Sample no.
−5.23	0.9992	203
	0.9992	204
	0.9993	207
−5.28	0.9992	211
−10.26	0.9979	203
	0.9981	204
−10.28	0.9982	207
	0.9981	211
−15.31	0.9962	207
	0.9961	211
−15.33	0.9961	203
	0.9962	204
−20.25	0.9934	211
−20.27	0.9933	203
	0.9933	204
−20.28	0.9934	207
−25.12	0.9895	203
	0.9893	204
−25.13	0.9893	207
−25.15	0.9894	211
	0.9894	219
	0.9894	220
	0.9894	221
−29.98	0.9839	216
	0.9840	217
	0.9840	218
−30.03	0.9839	219
	0.9837	220
	0.9840	221
−30.99	0.9825	216
	0.9826	217
	0.9824	218
−31.00	0.9825	219
	0.9824	220
	0.9825	221
−31.02	0.9823	207
	0.9823	211
−31.05	0.9822	203
	0.9823	204
−31.96	0.9812	217
	0.9811	218
−32.06	0.9808	219
	0.9807	220
	0.9809	221
−32.90	0.9796	217
	0.9796	218
−33.03	0.9790	220
	0.9792	221
−33.41	0.9786	218

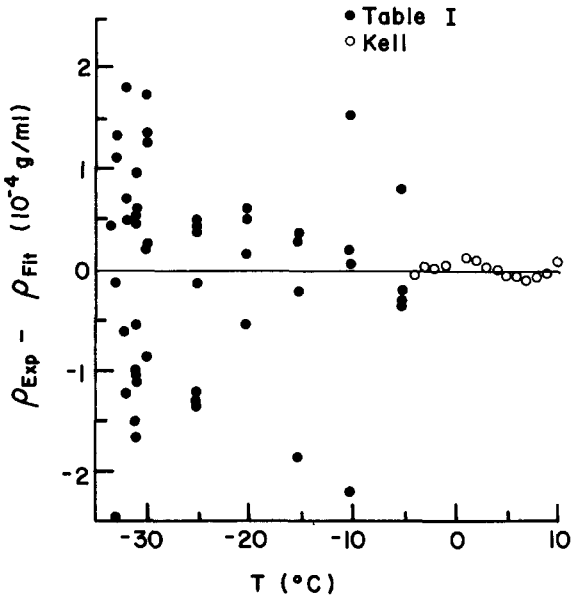

FIG. 2. Deviation plot of data relative to polynomial fit in Eq. (1).

$$\rho = \sum_{n=0}^{6} a_n t^n, \tag{1}$$

where ρ is the density in g/ml, t is the temperature in °C and $a_0 = 0.999\,86, a_1 = 6.690\times10^{-5}, a_2 = -8.486\times10^{-6}, a_3 = 1.518\times10^{-7}, a_4 = -6.9484\times10^{-9}, a_5 = -3.6449\times10^{-10}$, and $a_6 = -7.497\times10^{-12}$. The deviation of this fit compared to the data is displayed in Fig. 2. Figure 2 illustrates that the standard deviation in the data and in the fit is about $\pm 1\times10^{-4}$ g/ml. Some systematic deviation is seen in our fit relative to the Kell data but since it is much less than our experimental error, we did not try to improve the fit.

Numerical values of ρ from Eq. (1) are tabulated in Table II and may be considered the smoothed data result of this work. The expansivity, $\alpha = -\rho^{-1}(\partial\rho/\partial T)_p$, calculated from Eq. (1) is also tabulated in Table II.

Figure 3 compares our results to earlier work. This earlier work includes the data of Schufle and Venugopalan[8] using 4 and 10 μ i.d. capillaries, Zheleznyi[9] who used 4–18 μ i.d. capillaries, Sorensen[10] who used 60–90 μ i.d. capillaries, Hare and Sorensen[5] who used 25 μ i.d. capillaries, and Rasmussen and MacKenzie[11] who used an emulsion with average water droplet diameter of 3.5 μ. All capillary density data show larger densities than ours except those of Zheleznyi which do not follow the trend of the other capillary data.

Figure 3 suggests that the bulk water density is perturbed to larger values in small capillaries. To explore this perturbation further we plot the excess density, $\rho_{ex} = \rho(r) - \rho(\infty)$, in a capillary of inside radius r vs the capillary inside diameter ($2r$) on a log–log graph in Fig. 4. For $\rho(\infty)$, i.e., the bulk data, we use our results in Table II.

TABLE II. Smoothed density data

T(°C)	Density(g/ml)	Expansivity(10^{-4}K^{-1})
0.00	0.9999	−0.67
−1.00	0.9998	−0.84
−2.00	0.9997	−1.03
−3.00	0.9996	−1.23
−4.00	0.9994	−1.44
−5.00	0.9993	−1.66
−6.00	0.9991	−1.89
−7.00	0.9989	−2.14
−8.00	0.9987	−2.40
−9.00	0.9984	−2.68
−10.00	0.9982	−2.97
−11.00	0.9978	−3.27
−12.00	0.9975	−3.58
−13.00	0.9971	−3.91
−14.00	0.9967	−4.26
−15.00	0.9963	−4.61
−16.00	0.9958	−4.99
−17.00	0.9953	−5.38
−18.00	0.9947	−5.79
−19.00	0.9941	−6.22
−20.00	0.9935	−6.68
−21.00	0.9928	−7.16
−22.00	0.9921	−7.68
−23.00	0.9913	−8.23
−24.00	0.9904	−8.83
−25.00	0.9895	−9.47
−26.00	0.9886	−10.18
−27.00	0.9875	−10.95
−28.00	0.9864	−11.79
−29.00	0.9852	−12.72
−30.00	0.9839	−13.75
−31.00	0.9825	−14.90
−32.00	0.9809	−16.16
−33.00	0.9793	−17.57
−34.00	0.9775	−19.14

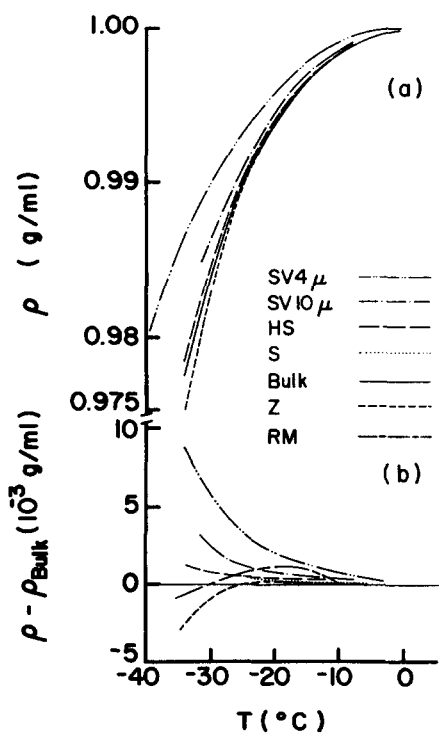

FIG. 3. Comparison of density measurements of earlier workers in various sample configurations. Part (a) absolute density values, part (b) values relative to the bulk data presented in this paper. Data used include Schufle and Venugopalan in 4 and 10 μ i.d. capillaries (SV4 μ and SV10 μ), Hare and Sorensen in 25 μ i.d. capillaries (HS), Sorensen in 60–90 μ i.d. capillaries (S), data in this work considered "Bulk," Zheleznyi in 4–18 μ i.d. capillaries (Z), and Rasmussen and MacKenzie with 3 μ diam emulsion droplets (RM).

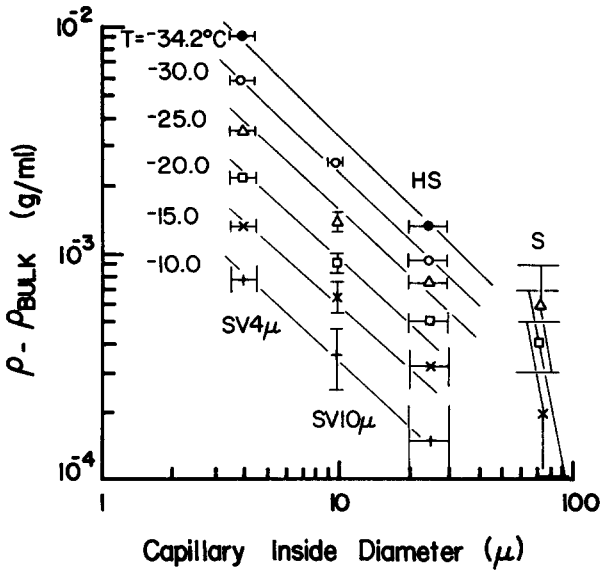

FIG. 4. Excess density, $\rho - \rho_{\text{bulk}}$, where ρ_{bulk} is the data presented in this paper (i.d. 300 μ) vs capillary inside diameter.

Error bars are large, but a linear, inverse dependence on radius is supported within the error by the linear dependence with slope of negative one for each temperature considered.

The data of Zheleznyi which were also obtained from capillaries do not follow this trend. We do not know why. His data show smaller densities for $T < -25$ °C than our bulk data and thus overestimate the anomaly in the expansivity as claimed by Leyendekkers and Hunter. The emulsion data of Rasmussen and MacKenzie show deviations relative to our bulk results, but we do not consider these deviations significant because they are comparable to their experimental error which was approximately 5×10^{-4} g/ml.

Leyendekkers and Hunter also described this density perturbation. They explained it in terms of an excess volume given by

$$V_{\text{ex}} = \left(\frac{\partial G_{\text{ex}}}{\partial p}\right)_T, \tag{2}$$

where G_{ex} is the excess surface Gibbs free energy and is given by

$$G_{\text{ex}} = \frac{2V\gamma}{r}. \tag{3}$$

Here V is the molar volume, γ is the interfacial tension, and r is the radius of curvature of a spherical drop. They then proceeded to apply Eq. (2) to Eq. (3) and obtained

$$V_{\text{ex}} = G_{\text{ex}}\left[\left(\frac{\partial \ln \gamma}{\partial p}\right)_T - \left(\frac{2}{3}\right)\kappa_T\right]. \tag{4}$$

Here $\kappa_T = -V^{-1}(\partial V/\partial p)_T$ is the isothermal compressibility. For a liquid drop the second term in Eq. (4) (except for the factor of 2/3) represents the compression of the drop due to the pressure differential across the drop given by the Kelvin equation

$$\Delta p = \frac{2\gamma}{r}. \tag{5}$$

For a capillary, the radius of curvature r of the meniscus is negative, hence this second term would yield positive V_{ex}, hence negative ρ_{ex} which is not observed. Thus they concluded that the first term in Eq. (4), due to the pressure derivative of γ, must become large and dominant in the supercooled regime to overwhelm the compression term and make $V_{\text{ex}} < 0$ hence $\rho_{\text{ex}} > 0$ (for capillaries where $r < 0$). Furthermore, the effect should vary inversely with radius as is observed.

We do not agree with this interpretation. First, as pointed out by Speedy,[12] no mechanical argument can justify the apparent compression of the water in capillaries due to a concave meniscus ($r < 0$). Second, one can in fact show that if the Leyendekkers and Hunter interpretation were correct, water would display a negative capillary rise (i.e., capillary depression) in the supercooled regime. We have qualitatively measured water's capillary rise in capillaries to -10 °C and saw no such behavior.

Third, consider the following thermodynamic argument to derive Eq. (3). The Gibbs energy and chemical potential μ for a single component system are related by

$$G = \mu N, \tag{6}$$

where N is the number of molecules. For a liquid drop in isothermal equilibrium with its gas, the chemical potential of the drop is a function of its pressure. The pressure inside the drop will be greater than the gas due to the surface tension. This pressure differential is given by the Kelvin equation, Eq. (5), with $\Delta p = p_l - p_g$ where p_l and p_g are the liquid and gas pressure. We now isothermally Taylor expand the liquid drop chemical potential at p_l, $\mu(p_l)$, about p_g to second order

$$\mu(p_l) = \mu(p_g) + \left(\frac{\partial \mu}{\partial p}\right)_T\Big|_{p=p_g} \Delta p + \frac{1}{2}\left(\frac{\partial^2 \mu}{\partial p^2}\right)_T\Big|_{p=p_g} \Delta p^2. \tag{7}$$

From $V/N = v = (\partial \mu/\partial p)_T$ and $\kappa_T = -V^{-1}(\partial V/\partial p)_T$ and the Kelvin equation, Eq. (7) can be rewritten as

$$\mu(p_l) = \mu(p_g) + v_l(p_g)\frac{2\gamma}{r} - \frac{1}{2}v_l\kappa_T\left(\frac{2\gamma}{r}\right)^2. \tag{8}$$

The second term in Eq. (8) is the excess Gibbs energy, Eq. (3), used by Leyendekkers and Hunter. To arrive at Eq. (4) one must assume $V_l = Nv_l$, γ, and r can all be differentiated with respect to p *independently*. That this is *not* true can be seen by closer examination of Eq. (7) which holds constraints on the variability of V_l, γ, and r. The proper method to find $V_l(p_l)$ is to differentiate Eq. (7) with respect to p_l to find

$$V_l(p_l) = V_l(p_g) - V_l(p_g)\kappa_T\frac{2\gamma}{r}. \tag{9}$$

Equation (9) displays the compression of the drop by $\Delta p = 2\gamma/r$ as expected by physical arguments. No erroneous $(\partial\gamma/\partial p)$ terms arise. It may be applied to capillary systems by using a negative r.

We now return to the excess density seen in the small capillaries. To explore this excess density effect further, we plot in Fig. 5 the coefficient A in

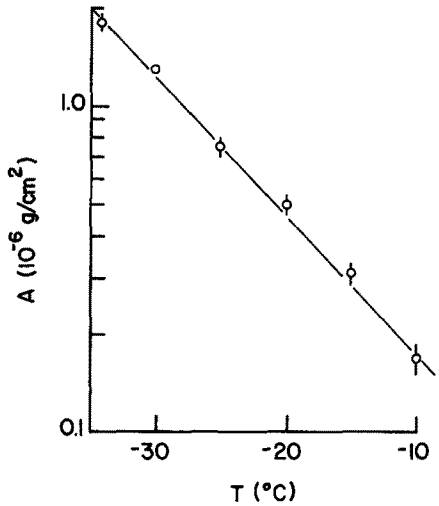

FIG. 5. Coefficient A of the "excess density effect" on water's density in capillaries of inside radius r where $\rho(r) - \rho(\text{bulk}) = A/r$.

$$\rho_{ex} = A/r. \tag{10}$$

The semilog nature of Fig. 5 demonstrates the exponential increase of A with decreasing temperature. Hence A could be said to behave anomalously at low temperature just as many other properties of supercooled water. Our attempts to fit A to a power law against $(T - T_s)$ where T_s is a singular temperature were not successful, however, requiring $T_s \simeq -100$ °C and then with $(T - T_s)$ spanning only a mere fraction of a decade.

What then is the cause of this large $\rho_{ex} \sim r^{-1}$ effect? Supercooled water has an open, hydrogen bonded network structure. If we may be allowed to speculate a moment, we point out that it is possible to make arguments wherein a surface layer with the density of nonhydrogen bonded water exists on the inside wall of the capillaries. If the layer's thickness is dependent only on temperature and not the capillary diameter, this argument leads to an inverse dependence of the excess density with capillary diameter but requires surface layers as large as several hundred angstroms thick at extreme supercoolings. Such a phenomenon seems very unlikely.

The excess density effect is reminiscent of the polywater era. Polywater, which is now considered a result of dissolution of silicates from the glass tubes, occurred in micron-sized tubes.[13] It might be that similar submicron surface layers have existed in the tubes in the references above which were used to uncover this effect. Both these speculations must await further experimental work before any further development of the cause of this effect can occur.

Regardless of our uncertainty regarding the source of the excess density effect in smaller capillaries, we can justify that our measurements presented here are free from these effects and represent bulk water data. This justification is given by extrapolation of the -34.2 °C line, the temperature for which the surface effect is a maximum, in Fig. 4 to $d \simeq 300\,\mu$ to find $\rho_{ex} \sim 10^{-4}$ g/ml which is within our experimental error. Thus we conclude that, within experimental error, our density measurements represent bulk water.

If A were accurately known at all temperatures, data obtained in smaller capillaries could be corrected for the excess density effects. While A is not known well, we can extrapolate its effect to correct Schufle and Venugopalan's $d = 4\,\mu$ capillary data which extend to -39.93 °C. We use Fig. 4 to extrapolate ρ_{ex} along $d = 4\ \mu$, to find ρ_{ex} $(T = -39.93\,°C,\ d = 4\ \mu) = (1.5 \pm 0.1) \times 10^{-2}$ g/ml. Schufle and Venugopalan found for $d = 4\ \mu$ and $T = -39.93$ °C, $\rho = 0.9806$ g/ml. Thus $\rho_{bulk} = 0.965 \pm 0.001$ g/ml at $T = -39.93$ °C. Extrapolation of the polynomial fit in Eq. (1) to -39.93 °C yields $\rho = 0.963$ g/ml which is in fair agreement with the corrected Schufle and Venugopalan value.

We now attempt to fit our expansivity results in Table II to a power law with $(T - T_s)$. As discussed in our earlier work, analysis of the expansivity α in terms of a power law is difficult because the background component of α, i.e., that normal α that would exist even if no anomaly were present, is poorly known. To determine the background expansivity α_B Leblond and Hareng[14] analyzed α for superheated H_2O in the range $160 < T < 220$ °C. Spectroscopic evidence indicates hydrogen bonding is small in this temperature range. They fit the data to a power law diverging at the gas–liquid spinodal and then extrapolated the fit to -40 °C, a rather long range extrapolation. Oguni and Angell[15] have estimated α_B from aqueous solution data and their results tend to bracket the Leblond-Hareng background. Leyendekkers[16] gives a form for α_B based on the background compressibility. This background seems to be more realistic at large temperatures. These backgrounds were displayed graphically in Fig. 3 of Ref. 5.

We fit our data to the form

$$\alpha_B - \alpha = \alpha_0 (T - T_s)^{-x}. \tag{11}$$

Values of α were obtained from Table II and, for $0 < T < 150$ °C, from Ref. 5. Using α_B from Leblond and Hareng, we could not obtain a linear fit on a log–log plot when all data in the $-33.4 < T < 150$ °C range here used. This poor fit may be due to the fact that $\alpha_B \to \alpha$ for $T > 100$ °C which seems unrealistic. If as in our earlier work we limit our range to $-33.4 < T < 55$ °C, a better fit is found with $T_s = -67$ °C, $x = -1.66$, and $\alpha_0 = 0.77\ \text{K}^{-1}$. The fit is displayed in Fig. 6. The value $x > 1$ seems unreasonable because it implies that $\rho \to 0$ as $T \to T_s$.

The fit using α_B from Leyendekkers is more successful. Using all data in the range $-33.4 < T < 150$ °C, we find a best fit with $T_s = -45$ °C, $x = 0.89$, and $\alpha_0 = 0.022\ \text{K}^{-1}$. This fit is also displayed in Fig. 6 and is seen to be quite good. The value of $T_s = -45$ °C corroborates the Speedy–Angell temperature which has been used to describe the singular behavior of many other properties of supercooled water.

The results of the expansivity analysis in terms of Eq. (11) must be judged, unfortunately, inconclusive. This is largely due to the uncertainty in α_B. It is noteworthy, however, that the most successful fit yielded $T_s = -45$ °C, the Speedy–Angell singular temperature. We must exercise temperance because of the small range of the power law fit, a decade and a half, and our inability to get closer than ~ 12 °C to the proposed singular temperature.

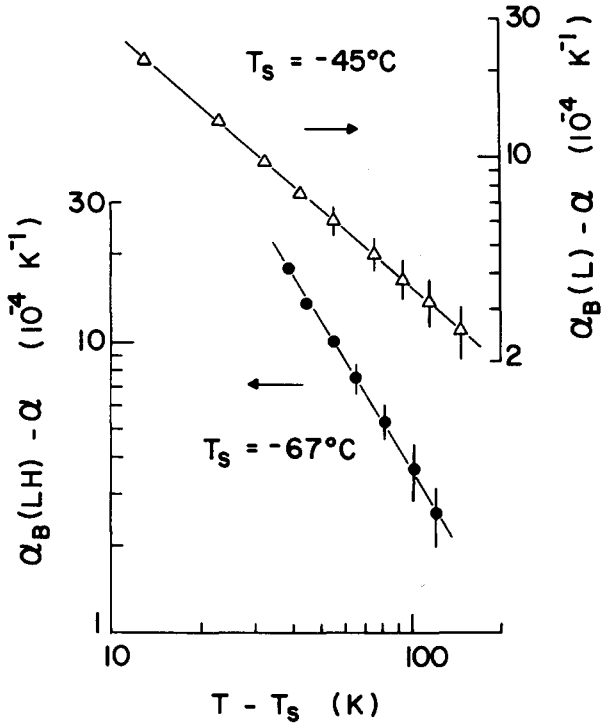

FIG. 6. Singular part of the expansivity, $\alpha_B - \alpha$ vs $T - T_s$, where T_s is a singular temperature. The data are shown with two different backgrounds: α_B(LH) is the Leblond and Hareng background (circles), and α_B(L) is the Leyendekkers background (triangles). Lines are best fits described in the text.

As a final point, we wish to describe the behavior of the density extrapolated to lower temperatures. It is a reasonable speculation that supercooled water is approaching a state wherein all the water molecules are completely hydrogen bonded to their neighbors to form a manifestly connected network. This network might be similar to ice Ih or amorphous water which have densities of 0.917 and 0.92 g/ml, respectively. Extrapolation of our polynomial fit in Eq. (1) to these densities occurs at a temperature of -48 to -49 °C which is comparable to the Speedy–Angell temperature and recent Raman data analysis.[17] While this long range extrapolation is dangerous, we feel it supports the concept that water is approaching some well connected state.

IV. CONCLUSION

Comparison of our density data obtained from 300 μ i.d. capillaries to earlier data obtained from measurements in smaller capillaries showed that the smaller capillary data were larger. This excess density in small capillaries was found to be inversely proportional to the capillary inside diameter and to increase exponentially with decreasing temperature. We can offer no explanation for this excess density, but we do show it is not a result of an excess surface free energy as proposed by Leyendekkers and Hunter. We saw above that our capillaries were large enough to avoid this excess density and hence yielded bulk water density data. Furthermore, nucleation at -33 °C for this size capillary represents the homogeneous nucleation temperature. Thus our data are the coldest possible bulk sample measurements for the density of liquid water. The bulk thermal expansivity derived from these data appears to behave anomalously and may be fit to a power law against $(T - T_s)^{-x}$. The fit is, however, inconclusive due in large part to ambiguity in the background expansivity. The most aesthetically pleasing fit, however, is quite linear in log–log space and yields a singular temperature of -45 °C, the Speedy–Angell temperature.

ACKNOWLEDGMENTS

We thank D.H. Rasmussen for supplying us with his emulsion density data. This work was supported by NSF Grant No. CHE-8219571.

[1] R. J. Speedy and C. A. Angell, J. Chem. Phys. **65**, 851 (1976).
[2] C. A. Angell, *Water, a Comprehensive Treatise*, edited by F. Franks (Plenum, New York, 1981), Vol. 7, Chap. 1.
[3] C. A. Angell, Annu. Rev. Phys. Chem. **34**, 593 (1983).
[4] J. V. Leyendekkers and R. J. Hunter, J. Chem. Phys. **82**, 1440, 1447 (1985).
[5] D. E. Hare and C. M. Sorensen, J. Chem. Phys. **84**, 5085 (1986).
[6] S. C. Mossop, Proc. Phys. Soc. London Sect. B **68**, 193 (1955)
[7] G. S. Kell, J. Chem. Eng. Data **12**, 66 (1967).
[8] J. A. Schufle and M. Venugopalan, J. Geophys. Res. **72**, 3271 (1967).
[9] B. V. Zheleznyi, Russian J. Phys. Chem. **42**, 950 (1968); **43**, 1311 (1969).
[10] C. M. Sorensen, J. Chem. Phys. **79**, 1455 (1983).
[11] D. H. Rasmussen and A. P. MacKenzie, J. Chem. Phys. **59**, 5003 (1973); (private communication).
[12] R. J. Speedy (preprint).
[13] D. H. Everett, J. M. Haynes, and P. J. McElroy, Sci. Prog. Oxford **59**, 279 (1971).
[14] J. Leblond and M. Hareng, J. Phys. (Paris) **45**, 373 (1984).
[15] M. Oguni and C. A. Angell, J. Chem. Phys. **78**, 7334 (1983).
[16] J. V. Leyendekkers, J. Chem. Soc. Faraday Trans. 1 **81**, 519 (1985).
[17] J. L. Green, A. R. Lacey, and M. G. Sceats, Chem. Phys. Lett. **130**, 67 (1986).